Assessing the potential of hybrid fossil–solar thermal plants for energy policy making: Brayton cycles

Eva Bernardos, Ignacio López *, Javier Rodríguez, Alberto Abánades

ETSI Industriales, Universidad Politécnica de Madrid (UPM), José Gutiérrez Abascal 2, 28006 Madrid, Spain

HIGHLIGHTS

- We model a generic solar–fossil hybrid Brayton cycle.
- We calculate the operating conditions for maximum ratio power/fuel consumption.
- Best hybrid plant conditions are not the same as solar or power blocks separately.
- We study potential for hybridization with current solar technologies.
- Hybridization at the Brayton in a combined cycle may achieve high power/fuel ratio.

ARTICLE INFO

Keywords:
Hybrid power plant
Energy efficiency
Tools for policy making

ABSTRACT

This paper proposes a first study in-depth of solar–fossil hybridization from a general perspective. It develops a set of useful parameters for analyzing and comparing hybrid plants, it studies the case of hybridizing Brayton cycles with current solar technologies and shows a tentative extrapolation of the results to integrated combined cycle systems (ISCSS). In particular, three points have been analyzed: the technical requirements for solar technologies to be hybridized with Brayton cycles, the temperatures and pressures at which hybridization would produce maximum power per unit of fossil fuel, and their mapping to current solar technologies and Brayton cycles. Major conclusions are that a hybrid plant works in optimum conditions which are not equal to those of the solar or power blocks considered independently, and that hybridizing at the Brayton cycle of a combined cycle could be energetically advantageous.

1. Introduction

On the consumer side, the current energetic scenario shows two opposing trends: an increasing demand pushing for greater power and, at the same time, a concern for the environment and for dependence on fossil fuels (Kaygusuz, 2012). As a consequence of this, there is a drive on the generation side toward a new paradigm, largely renewable-based, which would thus guarantee sustainability while satisfying the growing demand, and which would bring together the two previous opposing trends. A graphical summary of this vision is shown in Fig. 1.

Renewable energies could ideally solve or damp down the environmental and strategic problems of today's generation scheme, but in reality they present features that are slowing down their massive deployment (Suresh et al., 2010). Solar energy in particular depends on the availability of solar resource, the maturity of the associated technologies and, critically, on its cost. There already exist some very developed technologies (parabolic trough collectors for example), but solar plants still present a high investment cost, significantly higher with storage, and they achieve relatively low solar-to-electric efficiency in any case (Williges et al., 2010). Moreover, the working hours of solar plants happen around the central hours of the day. With energy storage, a plant could operate for some time after that, but this would still allow adjusting to the demand curve only slightly.

Perhaps at an intermediate stage between conventional and renewable paradigms, solar–fossil hybridization may be the way to a more economic, environment-friendly and reliable supply of electricity (Erdnic and Uzunoglu, 2012), and therefore a further step towards the new energetic scenario. From the point of view of economy and performance, hybrid have advantages over standalone solar plants: solar energy can be converted to electric energy at a higher efficiency (Dersch et al., 2004), and they require lower investment due to an adaptable solar share (Schwarzbözl et al., 2006) that allows having a smaller solar field for a nominal design power (Ávila-Martín, 2011). Furthermore, combining both solar

* Corresponding author. Tel.: +34 913363150; fax: +34 913364262.
E-mail addresses: ignacio.lopez@upm.es, ilopez@etsii.upm.es (I. López).

Nomenclature

c_p	specific heat
c_{pA}	specific heat at the compression stage
c_{pB}	specific heat at the heating stage
c_{pC}	specific heat at the expansion stage
e	error between simulation and theoretical values
η	efficiency of the Brayton cycle
η_{se}	solar electric efficiency
η_{sc}	isoentropic efficiency of compressor
η_{st}	isoentropic efficiency of turbine
ϕ	solar share
G_b	beam solar energy
h_x	specific enthalpy at point x
m_a	mass of air entering the cycle
m_c	mass of fuel entering the cycle
Q_T	total heat entering the Brayton cycle
Q_c	heat provided by the fossil fuel to the cycle
Q_s	heat provided by the solar field to the cycle
r	pressure ratio of the Brayton cycle
ρ_f	fossil coefficient of performance
T^i_{sol}	inlet temperature of the solar block
T^o_{sol}	outlet temperature of the solar block
ΔT_{HE}	temperature drop at the heat exchanger which couples solar and power blocks
W	power produced at the turbine
op	optimum operating conditions
'th'	superindex indicating a value obtained by a theoretical model

and fossil sources of energy is relatively straightforward from the technological point of view, because they share a large number of common parts; in fact, there already exist a number of hybrid plants. Two examples are the integrated solar combined cycle systems (ISCCS) at the Hassi R'Mel plant in Algeria (Behar et al., 2011), and the Yadz plant in Iran (Baghernejad and Yaghoubi, 2010).

It is therefore clear that hybridization should be considered in energy strategies (the interest of hybrid systems in developing countries (Chien and Lior, 2011; Horn et al., 2004), where primes to solar electricity production or funding support are limited, has been already observed (Kaygusuz, 2012; Suresh et al., 2010; Hosseini et al., 2005)). However, this would require understanding it fully, which means being able to design strategic plans and to estimate their effects.

Designing a strategy for large scale hybridization would involve selecting a number of advantageous alternatives among the full spectrum of possible hybrid topologies, and subsequently tailoring appropriate granting schemes and policies around them, based on their expected performance under different demand and climatic scenarios. Let us consider the summarized forecasting process of Fig. 2:

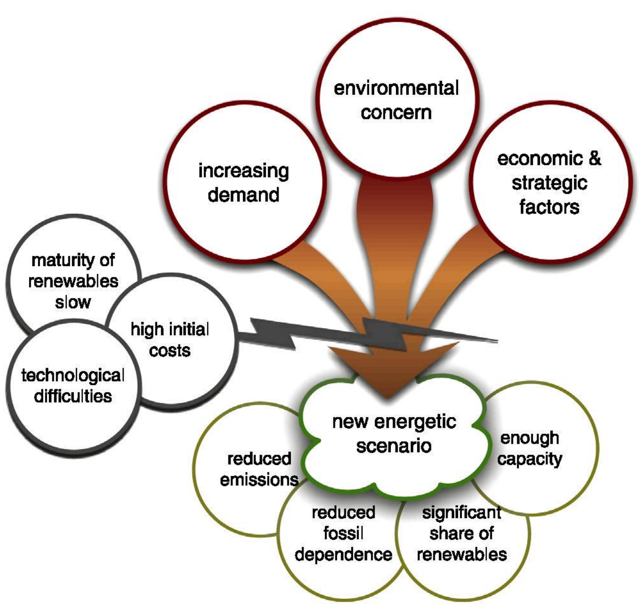

Fig. 1. Diagram describing the trends and factors in the current energetic scenario.

Step 1: A set of hybrid plants is chosen, either to be newly built or to be built by adapting existing ones. The type of hybrid plant is decided for each case: which is the conventional block, which solar technology will be associated to it.

Step 2: Throughout a day, a plant will typically operate in different conditions, ranging from minimum load to nominal power. Models of the hybrid plant for each type of operation estimate fuel consumption.

Step 3: The energy production of the plant must be integrated in time, throughout the hours of the day and the days of the year in order to calculate the yearly performance: total generated energy, fuel consumption, etc.

As of today, we do not know, for a given conventional plant, which will be the best way to integrate a solar contribution ('a' in the figure). We lack comparative studies between the possible combinations of conventional plants and solar technologies, and modes of hybrid operation. There do not exist comprehensive, systematic studies about the economy related to hybrid plants either, so there is no information for designing adequate energy regulations ('b' in the figure).

On the positive side, today we have enough experience with solar technologies and there exist the necessary tools to generate the studies needed for policy making. For instance, there exist specialized, simulation-based tools for analyzing specific hybrid systems (Erdnic and Uzunoglu, 2012). There also exists an heterogeneous series of studies of specific hybrid systems, from the economic point of view (Neij, 2008; Papineau, 2006), energy policy (Zhang et al., 2010), and in some technical aspects (Livshits and Kribus, 2011). Generally, existing studies have a restricted scope, limited to analyzing specific plants or components (Ávila-Martín, 2011; Heller et al., 2006). The main conclusion from this is that tools for policy making would require more general methodologies and broad-scope studies.

This paper intends to provide a contribution to point 'a' of Fig. 2, and addresses (more or less directly) the following questions:

- Which technical conditions must hold to be able to hybridize at all?
- Which solar–thermal technologies and devices should it be invested in?
- Although, in principle, any hybridization is good from the energy point of view, how could the most be obtained from it?
- Would it be advantageous to hybridize existing fossil-fuel plants?

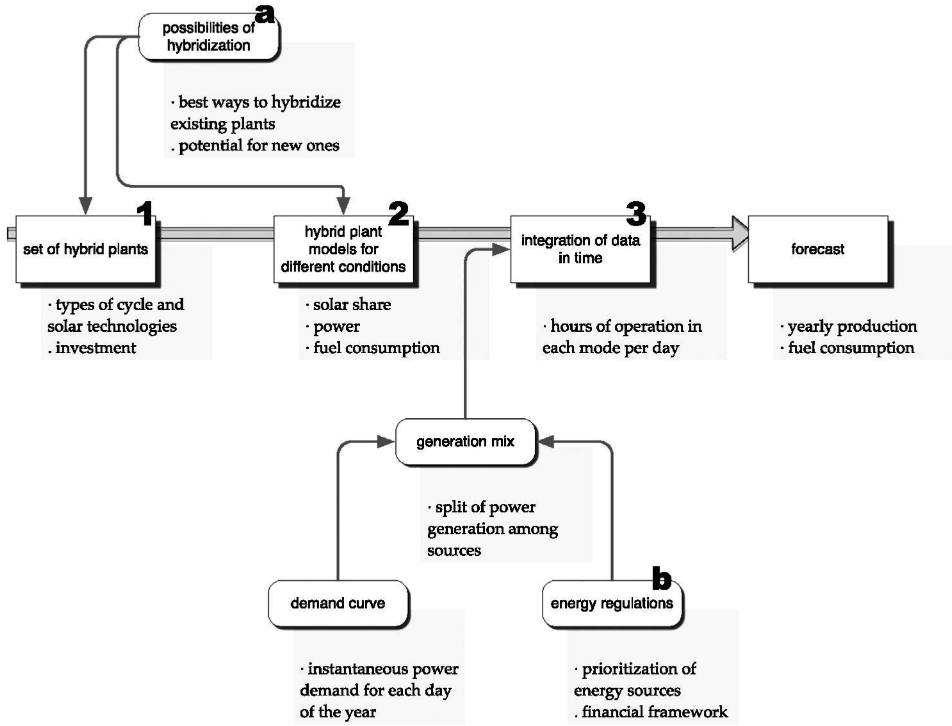

Fig. 2. Summary of a forecasting analysis including renewables. Steps of the main calculations are numbered 1–3, some related factors are labelled a and b.

- How should new plants be designed?

In particular, this paper analyzes the potential for hybridizing a generic Brayton cycle: when it could (or should not) be done, how much could be saved by doing it, and how it should be operated for optimum performance. The results of this paper would lead directly to the models of step 2 of the forecasting process of Fig. 2 for Brayton plants.

The paper has two parts: the first (Sections 2 and 3) assesses the thermodynamical problem. In the second, Section 4 provides a brief survey of the current solar thermal technologies and applies the previous results to them in order to evaluate their potential for hybridization. Section 5 develops a short extrapolation of this study from Brayton to combined cycles and a brief discussion on solar efficiency. Finally, Section 6 concludes the major ideas of the work.

2. Methodology

This study is based on the typical simplified scheme of a hybrid Brayton cycle of Fig. 3, which will be described in detail in Section 2.1. The model abstracts particular, implementational aspects in order to signify the general behaviour of the cycle.

Some parameters have been defined to describe how the solar and power blocks are combined, and their joint performance. They are explained in Section 2.2.

The study consists of calculating the temperature and pressure for the points indicated in Fig. 3, which maximize the power produced at the turbine per unit fossil energy. This has been done in two ways:

- By simulating the plant across a range of operating conditions and then selecting the best set. The series of simulations were carried out with Engineering Equation Solver, EES (Klein, 2002).
- By considering a simplified analytical model of the plant and calculating the optimum. The simplifying hypotheses are explained in detail in Section 3.

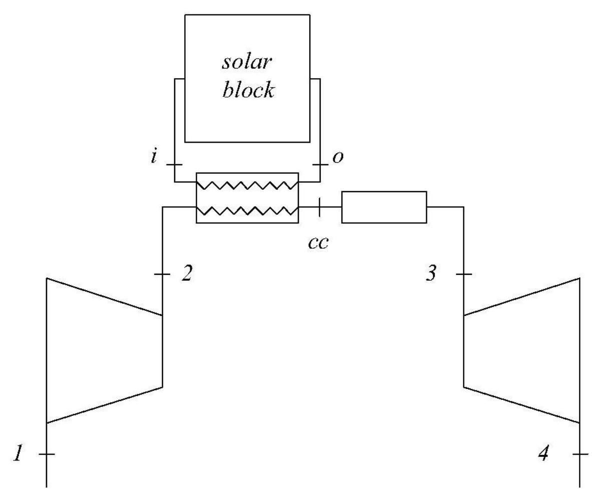

Fig. 3. Hybrid solar-Brayton system.

The purpose of the second study was to obtain simple expressions, if possible, which would allow understanding the relative influence of the plant design parameters in its performance, better than large series of simulation data. It was eventually found that the differences between simulation and analytical results fell within $\pm 10\%$, sufficient for the qualitative purpose of the paper. Figs. 6 and 7 show simulation results, but Section 3 will develop the analytical model.

2.1. Model of the solar-Brayton hybrid cycle

The enthalpy–entropy diagram of the Brayton cycle is shown in Fig. 4. The air enters the compressor at $T_1 = 288,15$ K, $P_1 = 1$ bar, where its pressurized to P_2 with an isentropic efficiency of $\eta_C = 0.845$. The pressure ratio, $r = P_2/P_1$, will be studied in the range $r \in [6, 35]$. The air leaving the compressor at point 2, enters

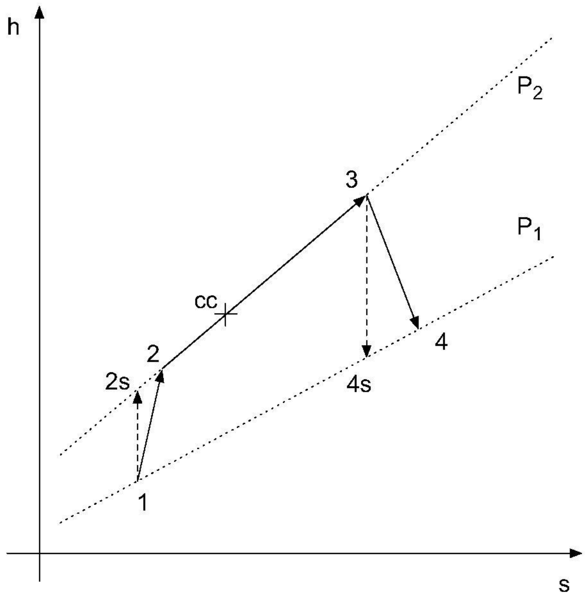

Fig. 4. Simplified thermodynamic diagram of the Brayton cycle.

the heat exchanger that couples the Brayton cycle to the solar block, where it pre-heats up to T_{cc}. It then enters the combustion chamber, where it mixes and reacts with the fuel. The combustion products enter the turbine at point 3. T_3 will be studied in the range $[1100, 1700]$K. Work is produced at the turbine, with isentropic efficiency $\eta_C = 0.845$, and finally leave the cycle at 4.

It is worth remarking that the ranges for r and T_3 have been fixed according to Boyce (2002) after revising the technological specifications of commercial gas turbines. In some cases the solar block could restrict them further; for example, r should not exceed 20 if pre-heating the air directly through a solar tower.

To model the solar block, the generic, black-box indicated in Fig. 3, will suffice, as long as its inlet and outlet temperatures, T^i_{sol}, T^o_{sol}, are known. The study is based on the energy that the field provides, therefore regardless of how it is implemented. Implementational characteristics of the field, especially its efficiency, have influence on the investment costs and on solar efficiency, as is outlined in Section 5.1.

The power and solar blocks are coupled *indirectly* by using a heat exchanger, as it can be observed in Fig. 3. The heat transfer fluid in the solar field and the thermal cycle fluid are assumed different, so, in general: $T_{cc} \approx T^o_{sol} - \Delta T_{HE}$, where ΔT_{HE} is the temperature drop at the exchanger, typically 10–20 K. Therefore, the limiting parameter for hybridization is the maximum T^o_{sol} that the solar technology may achieve.

When using some solar technologies, a solar tower for instance, the solar and power blocks could be coupled *directly*, without the heat exchanger of Fig. 3, by circulating the same fluid, air, through the solar and power blocks, making $T^o_{sol} \approx T_{cc}$.

2.2. Parameters and concepts of hybrid systems

The following parameters can be used to characterize a fossil–solar hybrid system:

- The *efficiency of the cycle, (η)*, defined as

$$\eta = \frac{W}{Q_T} \tag{1}$$

W is the net power produced by the cycle and Q_T the total energy input to the cycle. $Q_T \approx m_a(h_3 - h_2)$ if we consider $m_c \ll m_a$, being m_a and m_c the air and fuel mass flows respectively.

- *Solar share* (ϕ), the share of solar energy in the total energy input to the cycle (solar energy, Q_s, and fossil fuel energy, Q_c):

$$\phi = \frac{Q_s}{Q_T} = \frac{Q_s}{Q_s + Q_c} \tag{2}$$

According to Fig. 3, assuming $m_c \ll m_a$ and $h \approx h(T)$:

$$\phi = \frac{Q_s}{Q_T} \approx \frac{h_{cc} - h_2}{h_3 - h_2} \tag{3}$$

- *Fossil coefficient of performance* (ρ_f), net power produced by the cycle per unit fossil fuel energy:

$$\rho_f = \frac{W}{Q_c} \tag{4}$$

Some authors as in Suresh et al. (2010) use this concept, although it is called *energy efficiency*. However, we would rather distinguish it from the actual efficiency, η, because it is a somewhat different concept. It is interesting to observe the relation between them:

$$\rho_f = \frac{W}{Q_c} = \frac{W}{Q_T - Q_s} = \frac{\frac{W}{Q_T}}{1 - \frac{Q_s}{Q_T}} = \frac{\eta}{1 - \phi} \tag{5}$$

In a conventional cycle, $\phi = 0 \Rightarrow \rho_f = \eta$.

ρ_f is directly related to fuel consumption, the main running cost of the plant. It is therefore a direct measure of solar hybridization potential.

- *Solar–electric efficiency*, (η_{se}). The product of the net power and the solar share shall be called *solar work*, W_s. The solar–electric efficiency is the ratio between W_s and G_b, the beam solar energy, therefore the efficiency of the collector field is $\eta_s = Q_s/G_b$:

$$\eta_{se} = \frac{Q_s}{Q_T} W \cdot \frac{1}{G_b} = \eta_s \eta \tag{6}$$

- *Point of optimum hybrid performance, op*. The operating conditions of the hybrid plant at which ρ_f is maximum. Normally it will be given by r^{op} (pressure ratio), T_3^{op} (turbine inlet temperature) and ϕ^{op} (solar share). Although variables describing the solar field could be used instead of ϕ, this was preferred because it abstracts implementation-specific details and is therefore more general.

3. Design cases and generic results

There are two possibilities when designing a hybrid plant:

- An existing Brayton cycle wants to be hybridized, therefore r and T_3 are fixed. Then, for a given ϕ, the problem consists of calculating the necessary T_{cc}. From this, the temperature that must be provided by the solar field follows, T^o_{sol}.
- Either a solar block (or a plan for it) already exists, or a particular collector technology has been selected, so that the value of T^o_{sol} is fixed. A Brayton cycle for maximum ρ_f must be designed by calculating the values of r and T_3.

A short remark on T_2 must be made. Air heats up to T_2 in the compression from P_1 to P_2. The solar block must allow heating it further, so that $T_{cc} \geq T_2$ (see Fig. 3). In the second design case, there would appear a maximum value of r that would allow this condition to hold.

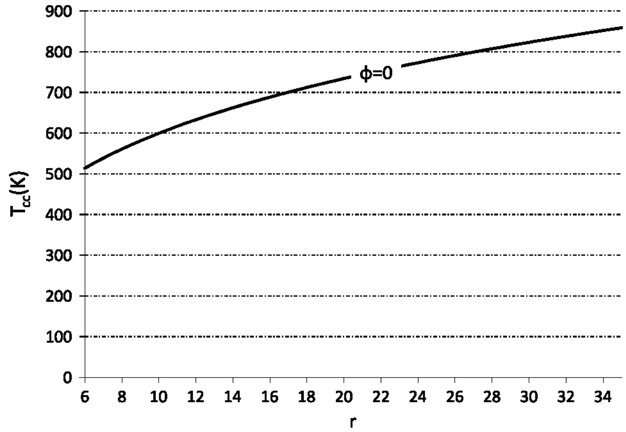

Fig. 5. Values of $T_2 = T_{cc}$ versus pressure ratio for a null solar share $\phi = 0$.

Of course, the limit condition for hybridization is $T_{cc} = T_2$, for which the solar share would be zero: $\phi = 0$. This condition is represented against pressure ratio in Fig. 5. Higher values of T^o_{sol} would imply higher T_{cc} and therefore greater ϕ.

3.1. T^o_{sol} for a given Brayton cycle

Let us consider a Brayton cycle defined by a certain (r, T_3) with efficiency η, which is to be hybridized at a certain ϕ. If follows from (5):

$$\rho_f = \frac{\eta}{1-\phi} \quad \in [\eta, \infty)$$

For a given ϕ, maximum ρ_f is reached at maximum efficiency operating conditions, so that $\eta = \eta^{max}$ (real cycles usually operate at slightly lower values); therefore ρ_f improves, the higher ϕ. The necessary T_{cc} for a desired ϕ and a given pressure ratio and turbine inlet temperature, $T_{cc} = T_{cc}(r, T_3, \phi)$, can be formulated by assuming constant $c_p = c_{pA}$ during stages 1 and 2, and analogously for stages 2 and 3, $c_p = c_{pB}$. Then, T_2 is derived from the definition of the isentropic efficiency:

$$\eta_{sc} = \frac{h_{2s} - h_1}{h_2 - h_1} \Rightarrow T_2 = T_1 + \frac{T_{2s} - T_1}{\eta_{sc}}$$

on the other hand:

$$\Delta s_{1-2s} = 0 \Rightarrow T_{2s} = T_1 r^{R/c_{pA}} \Rightarrow$$

$$T_2 = T_1\left[1 + \frac{1}{\eta_{sc}}\left(r^{r/c_{pA}} - 1\right)\right] \tag{7}$$

finally:

$$\phi = \frac{h_{cc} - h_2}{h_3 - h_2} \Rightarrow T_{cc} = \phi \cdot T_3 + T_2(1-\phi) \Rightarrow$$

$$T_{cc} = \phi \cdot T_3 + T_1(1-\phi)\left[1 + \frac{1}{\eta_{sc}}\left(r^{R/c_{pA}} - 1\right)\right] \tag{8}$$

It is not necessary to calculate c_{pB} because it cancels in the intermediate operations. Applied to our Brayton cycle, $c_{pA} =$ 1.035 kJ/kgK, R=0.2867 kJ/kgK. As a numerical example, Fig. 6 represents T_{cc}, and ρ_f as a function of ϕ and T_3 for Brayton cycles operating at η^{MAX} conditions.

Let us imagine a Brayton cycle operating at $T_3 = 1300$ K and r=17.7, that wants to be hybridized with $\phi = 0.15$. The fossil coefficient of performance of the hybrid plant would be $\rho_f = 0.35$, greater than the conventional by 20.6%. The required T_{cc} according to Fig. 6 is $T_{cc} \approx 800$ K.

As mentioned in the previous sections, in the case of indirect heat transfer, T^o_{sol} should be a typical 10–20 K higher than T_{cc}. In our case 810–820 K. The solar technologies that allow this temperature are shown in Table 1.

3.2. Optimal r, T_3 and ϕ for a given solar technology

In case the solar technology is given, values (or a range) for T^o_{sol} and T_{cc} are known. The problem consists of calculating r^{op} and T_3^{op}, for maximum ρ_f.

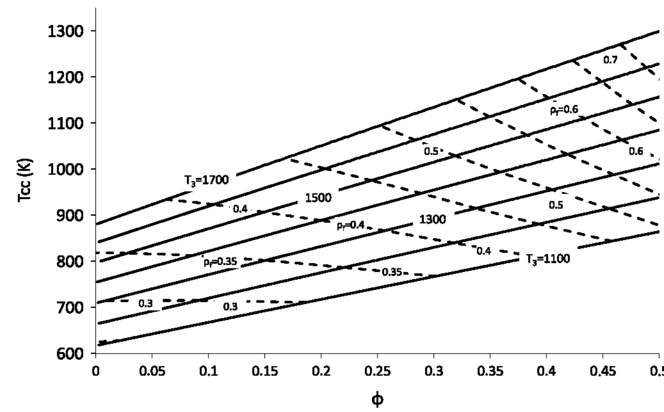

Fig. 6. Values of T_{cc} for maximum fossil coefficient of performance as a function of ϕ and T_3.

Table 1
Major solar–thermal technologies.

Technology	Notation	Heat transfer fluid	T^o_{sol}(K)	Status
Parabolic trough	CCP1	Thermal oil	666	Commercial
	CCP2	Water/steam (DSG)	823	Prototype
	CCP3	Molten salts	823	Commercial
Solar tower	RC1	Molten salts	838	Commercial
	RC2a	Air (atmospheric)	973	Prototype
	RC2b	Air (compressed)	1273	Prototype
	RC3a	Water/saturated steam	523	Commercial
	RC3b	Water/superheated steam	823	Commercial
	RC4	CO_2	873	Experimental
	RC5	Particles	1273	Experimental
Fresnel linear	F1	Water/steam	543	Commercial
	F2	Molten salts	823	Prototype
	F3	Superheated steam	773	Prototype

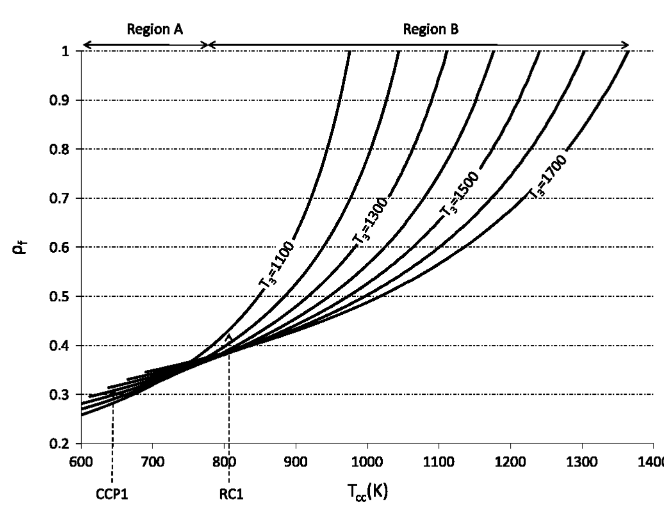

Fig. 7. Optimum hybridization as a function of T_{cc}.

Establishing the optimal ϕ requires a somewhat complex procedure:

1. Calculate an optimal T_3.
2. Calculate r^{op}.
3. Calculate the corresponding ϕ^{op}.

These three steps are not direct. T_3 results from reading the curves of ρ_f^{op} that will be discussed in Section 3.2.1. For calculating r^{op}, ρ_f must be formulated previously as explained in Section 3.2.2. r^{op} results by derivating this expression with respect to r, as shown in Section 3.2.3. With this value ϕ^{op} can finally be obtained, as shown in Section 3.2.4.

3.2.1. Turbine inlet temperature, T_3: design regions

The relation between T_{cc} and the optimal value of T_3 can be deduced from Fig. 7. The curves of ρ_f^{op} cross in the interval of T_{cc} between 725 and 775 K. This distinguishes two design regions:

- In region A, for a given T_{cc}, ρ_f^{op} increases as T_3 increases and ϕ is reduced. Hence, hybridization is not interesting because there exists a non-hybrid Brayton cycle ($\phi = 0$) of greater efficiency (and greater T_3).
- In region B, for a given T_{cc}, ρ_f^{op} increases as T_3 decreases and ϕ increases. This is the region in which hybridization may result interesting, because it allows using lower temperature turbines.

3.2.2. Formulation of ρ_f

It must be remarked that ρ_f in this case depends both on ϕ and η (not only on ϕ as in Section 3.1). From expressions (5) and (3), it follows $\rho_f = \rho_f(r, T_3, T_{cc})$. Given that T_{cc} is fixed, the problem is to find a relation between r and T_3 that maximizes ρ_f for the given T_{cc}:

$$\rho_f = \frac{h_3 - h_4 - (h_2 - h_1)}{h_3 - h_{cc}}$$

the compressor:

$$\eta_{sc} = \frac{h_{2s} - h_1}{h_2 - h_1}; \quad \Delta s_{1,2s} = 0 \Rightarrow$$

$$h_2 - h_1 = \frac{c_{pA}}{\eta_{sc}} T_1 \left(r^{R/c_{pA}} - 1 \right)$$

the turbine:

$$\eta_{st} = \frac{h_3 - h_4}{h_3 - h_4 s}; \quad \Delta s_{3,4s} = 0 \Rightarrow$$

$$h_3 - h_4 = \eta_{st} c_{pC} (T_3 - T_{4s}) = \eta_{st} c_{pC} T_3 \left(1 - r^{-R/c_{pC}} \right)$$

combining the previous:

$$\rho_f = \eta_{st} \frac{c_{pC}}{c_{pB}} \frac{T_3}{T_3 - T_{cc}} \left(1 - r^{-R/c_{pC}} \right) - \frac{1}{\eta_{sc}} \frac{c_{pA}}{c_{pB}} \frac{T_1}{T_3 - T_{cc}} \left(r^{R/c_{pA}} - 1 \right) \tag{9}$$

It can be observed that (9) is the desired expression $\rho_f = \rho_f(r, T_3, T_{cc})$. Specific heat has been assumed constant by intervals, in 1–2 c_{pA}, in 2–3 c_{pB} and in 3–4 c_{pC}.

3.2.3. Pressure ratio, r

The optimal pressure ratio for each value of T_{cc} and T_3 can be calculated from (9)

$$\left. \frac{\partial \rho_f}{\partial r} \right|_{T_3, T_{cc}} = \eta_{st} \frac{R}{c_{pB}} \frac{T_3}{T_3 - T_{cc}} r^{-(1 + R/c_{pC})} - \frac{1}{\eta_{sc}} \frac{R}{c_{pB}} \frac{T_1}{T_3 - T_{cc}} r^{(R/c_{pA} - 1)} = 0 \Rightarrow$$

$$r^{th} = \left(\eta_{st} \eta_{sc} \frac{T_3}{T_1} \right)^{\frac{c_{pA} c_{pC}}{R(c_{pA} + c_{pC})}} \tag{10}$$

The obtained pressure ratio is obviously a maximum as

$$\left. \frac{\partial^2 \rho_f}{\partial r^2} \right|_{T_3, T_{cc}} < 0 \tag{11}$$

3.2.4. Solar share, ϕ

It is possible to obtain an estimate of the solar share derived from the previous parameters and the theoretical value of T_2 worked out from (7)

$$\phi = \frac{h_{cc} - h_2}{h_3 - h_2} \approx \frac{T_{cc} - T_2}{T_3 - T_2} \tag{12}$$

3.3. Simulations and analytical model

The analytical model considers constant specific heat for each of the three stages of the Brayton cycle: c_{pA} (compression), c_{pB} (heating) and c_{pC} (turbine expansion). This allows to formulate the entropy increment between the final state, f, and the initial, i, as

$$\Delta s = \int_i^f \frac{c_p}{T} dT + \left(\frac{\partial s}{\partial P} \right)_T dP \approx c_p \ln \frac{T_f}{T_i} - R \ln \frac{P_f}{P_i}$$

Thus, the isoentropic outlet temperature of the compressor and the turbine can be worked out easily. Also, the definition of isoentropic efficiency of the turbine (analogously for the compressor), allows establishing a simple relation between the isoentropic and real outlet temperatures:

$$\eta_{st} = \frac{h_3 - h_4}{h_3 - h_{4s}} = \frac{\int_4^3 c_p \, dT}{\int_{4s}^3 c_p \, dT} \approx \frac{c_{pC}(T_3 - T_4)}{c_{pC}(T_3 - T_{4s})} = \frac{T_3 - T_4}{T_3 - T_{4s}}$$

As it was mentioned in Section 2, this model was developed only with the intention of allowing a clear understanding of the factors intervening in the hybrid parameters. Non-constant expressions, $c_p(T)$, and enthalpy adjustments, $h = h(T)$ which were also tested, would obscure the physical meaning of the model. The gain in accuracy would be $\leq 10\%$, which, given the qualitative nature of the study, did not justify the added complexity.

It must be remarked, however, that a first version of the simplified model considered a unique value for c_p, instead of the three presented here, yielding significantly poorer results (errors greater than 20%). The main reasons for this were that a single value would make the ratio $c_{pA}/c_{pB} \approx 1$ in (9), approximately 1.12 times its real value, and that the exponent in (10) would approximately double its real value. The full range of temperatures considered in this study is so large that a single average value for c_p cannot be representative.

4. Results: application to current solar technologies

Some solar technologies may have restrictions for being hybridized with a Brayton cycle due to temperature limitations, or may not be suitable all together. This section analyzes very briefly how the current technologies (Table 1) could be hybridized.

Oil is the most common heat transfer fluid for parabolic troughs (Fernández-García et al., 2010) (CCP1). Due to the upper temperature limit at 393 °C, other options reaching up to 500 °C are being investigated, such as direct steam generation, DSG (CCP2) (Zarza, 2003; Zarza et al., 2006; Eck et al., 2008) and molten salts (CCP3) (ENEA, 2011).

Solar tower technologies may use molten salts (RC1), atmospheric (RC2a) and compressed air (RC2b), and water. Prototypes of solar tower with compressed air have reached up to 1000 °C at 15–19 bar (Ávila-Martín, 2011), and could be coupled to a Brayton cycle directly. Lower temperatures have been achieved with water-steam technologies, in a range from 250 °C (Osuna et al., 2004) up to 565 °C (BrightSource, 2011).

The current Fresnel technology usually operates below 270 °C (Solar Power and Chemical Energy Systems, 2011), making it unsuitable for Brayton hybridization. Recently, superheated steam

Table 2
Application of the study to the current major solar thermal technologies. The table indicates fossil coefficient of performance. The corresponding value of ϕ is indicated below.

Technology	T_3 (K)						
	1100	1200	1300	1400	1500	1600	1700
CCP1	0.286	0.2936	0.3017	0.3101	0.318	–	–
	0.2	0.13	0.08	0.04	0.01	–	–
CCP2/CCP3/RC3b/F2	0.4334	0.4053	0.3925	0.3871	0.3854	0.3859	0.3877
	0.47	0.37	0.29	0.23	0.18	0.14	0.11
RC1	–	0.4377	0.417	0.4067	0.4019	0.4002	0.4004
	–	0.42	0.34	0.27	0.22	0.17	0.14
RC2a	–	–	–	0.53	0.4996	0.482	0.4706
	–	–	–	0.44	0.37	0.31	0.26
RC2b	–	–	6.65	1.754	1.15	0.9	0.78
	–	–	0.95	0.83	0.72	0.63	0.56
RC4	–	0.4625	0.4352	0.4211	0.4138	0.4104	0.4093
	–	0.45	0.36	0.29	0.24	0.19	0.15
RC5	–	–	4.43	1.56	1.069	0.86	0.76
	–	–	0.93	0.81	0.7	0.61	0.54
F1	0.2528	–	–	–	–	–	–
	0.03	–	–	–	–	–	–
F3	0.3718	0.361	0.3579	0.3584	0.3608	0.3644	0.3685
	0.38	0.29	0.22	0.17	0.13	0.09	0.06

at 500 °C has been achieved (Novatec Solar, 2011); even at higher temperatures with molten salts (Grena and Tarquini, 2011).

Table 2 shows the values of η_{fossil}^{max} and the corresponding ϕ for a Brayton cycle combined with each solar technology. It has been assumed that $T_{cc} = T_{sol}^{o} - 15$ K (in all cases except RC2b). Cases not suited for hybridization have been omitted.

For the case of parabolic troughs with thermal oil, CCP1, we may observe that, as in a non-hybrid Brayton, efficiency improves the higher T_3, because the T_{cc} is too low and falls within design region A (see Section 3.2.1). The rest of cases with parabolic troughs (water/steam and molten salts), CCP2 and CCP3, have T_{cc} values within region B, and therefore reach higher values of ρ_f at lower values of T_3. Analogous results are obtained with water-superheated steam solar tower, RC3b, and Fresnel with molten salts, F2. It can be observed that the rest of solar tower options follow the same trend. Fresnel technology using water-steam, F1, could allow hybridization in one only case, which would fall within design region A and should therefore be discarded; with superheated steam, however, Fresnel technology falls at the lower limit of design region B.

5. Discussion: solar–electric efficiency and ISCCS

5.1. Solar–electric efficiency

One of the drives toward solar–fossil hybridization is the increase of solar–electric efficiency. It is interesting to see that the best ρ_f is not obtained when the solar–electric efficiency is maximum.

From (6), we may deduce that, for a given collector field, the maximum solar–electric efficiency would require the Brayton cycle to be working at its maximum efficiency: $\eta_{se}^{max} = \eta_s \eta^{max}$. However, maximum ρ_f is obtained when operating at different conditions, therefore $\eta^{op} < \eta^{max}$. If we now take (6), it follows:

$$\eta_{se}^{op} = \eta_s \eta^{op} < \eta_s \eta^{max} = \eta_{se}^{max} \tag{13}$$

So, the best ρ_f is not obtained when the solar–electric efficiency is maximum nor when the Brayton efficiency is maximum either.

5.2. Brayton hybridization in ISCCS

Many of the Brayton cycles for electric generation are part of a combined cycle. It is interesting to study how an hybridization of the top cycle (Brayton) would affect the ρ_f of a combined cycle. Let us formulate the efficiency of a conventional combined cycle as

$$\eta_{comb} \approx \frac{W_B + W_R}{m_a(h_3 - h_2)} \tag{14}$$

where W_B and W_R are the power produced by the Brayton and Rankine cycles respectively. If the Brayton were hybridized, ρ_f would result (see Section 3.1):

$$\rho_{f,comb} \approx \frac{W_B + W_R}{m_a(h_3 - h_{cc})} = \frac{W_B + W_R}{m_a(h_3 - h_2)} \frac{(h_3 - h_2)}{(h_3 - h_{cc})} = \eta_{comb} \frac{1}{1 - \phi} \tag{15}$$

The improvement of ρ_f is by a factor of $1/(1-\phi)$, the same as it would be in the case of the Brayton on its own (5). This would mean that modifying the top, Brayton cycle would improve the whole cycle by the same ratio.

Although promising, this result is not conclusive, because the hybridization of a combined cycle is significantly more complex than that of a Brayton, and the case above only represents one among many possibilities. A combined cycle would admit combining the solar input at the top cycle (the option commented above), at the bottom cycle or in both cycles, in a given proportion. Note that for hybridizing at the bottom cycle, it should be repowered by an arbitrary factor, which adds an extra degree of freedom to the problem.

The bottom cycle itself would admit receiving solar energy at the economizer, the evaporator or the superheater in either of the pressure levels; at the preheaters, thus eliminating extractions at the steam turbine, or by having part of the water bypass the heat recovery steam generator and circulate through a separate exchanger with the solar field, as in Baghernejad and Yaghoubi (2010).

These considerations added to the practical issues introduced in Section 4 could actually mean that hybridizing a combined cycle at the top cycle could prove off-optimum technically, economically or both, depending on the solar technology and the actual hybridization option considered.

6. Conclusions

This paper proposes a first in-depth study of solar–fossil hybridization from a general perspective. It develops a set of useful technical tools for analyzing hybrid plants, it studies the case of hybridizing Brayton cycles with current solar technologies and shows a tentative extrapolation of the results to integrated combined cycle systems (ISCSS).

The following generic parameters allow describing a hybrid plant in a way that enables comparison between alternative plant configurations and that is meaningful for energy policy making: solar share, ϕ, fossil coefficient of performance ρ_f, solar–electric efficiency, η_{se} and point of optimum hybrid performance, *op*.

The results presented here are necessary for assessing the impact of potential hybridization policies. On one side they explain and summarize the technological requirements for hybridizing a Brayton cycle with current solar technologies. On the other, they allow calculating the optimum performance conditions of a hybrid Brayton plant. These results are useful in two ways:

- They allow valuating the potential of each of the current solar technologies for hybridization on a technical basis.
- They allow selecting a solar technology for hybridizing a specific Brayton plant, and estimating the resulting energetic performance.

This information can be used both for estimating the impact of possible hybridization deployment strategies, and for designing related economic measures.

Some of the current solar technologies, such as parabolic trough collectors with molten salts, could be used for hybridization with Brayton cycles. Others may still require some degree of research and development. However, hybridization is technically possible.

In combined cycle plants, even the relatively straightforward hybridization at the top, Brayton cycle outlined here could prove advantageous, because it would increase the fossil coefficient of performance of the whole plant by the same factor as that of the Brayton alone.

The work presented here must be completed with other theoretical studies in order to build a comprehensive set of tools for policy making, as well as to cover the entire spectrum of possible hybridization cases. Extending this study to the Rankine cycle could prove particularly interesting, as it would enable a full assessment of combined cycles and also cover coal plants. Another aspect yet to be analyzed is partial load operation.

Hybridization studies should be complemented by economic analyses, which would allow not only to assess the potential benefit of hybrid against conventional generation, but also to discriminate between the different possible technical solutions to a particular hybridization design problem. A full economic assessment of a hybrid plant should consider generation throughout a year, by integrating demand and generation curves, given that the solar resource is intrinsically time-dependent.

References

Ávila-Martín, Antonio L., 2011. Volumetric receivers in solar thermal power plants with central receiver system technology: a review. Solar Energy 85 (5), 891–910.

Baghernejad, A., Yaghoubi, M., 2010. Exergy analysis of an integrated solar combined cycle system. Renewable Energy 35 (10), 2157–2164.

Behar, Omar, Kellaf, Abdallah, Mohamedi, Kamal, Belhamel, Maiouf, 2011. Instantaneous performance of the first integrated solar combined cycle system in algeria. Energy Procedia 6 (0), 186–194.

Boyce, Meherwan P., 2002. Gas Turbine Engineering Handbook, 2nd edition. Gulf Professional.

BrightSource, 2011. SEDC Project. ⟨http://www.brightsourceenergy.com/projects/sedc/⟩.

Chien, John Chung-Ling, Lior, Noam, 2011. Concentrating solar thermal power as a viable alternative in China's electricity supply. Energy Policy 39 (12), 7622–7636. (Clean Cooking Fuels and Technologies in Developing Economies).

Dersch, Jürgen, Geyer, Michael, Herrmann, Ulf, Jones, Scott A., Kelly, Bruce, Kistner, Rainer, Ortmanns, Winfried, Pitz-Paal, Robert, Price, Henry, 2004. Trough integration into power plants—a study on the performance and economy of integrated solar combined cycle systems. Energy 29 (5–6), 947–959.

Eck Markus, Bahl Carsten, Bartling Karl-Heinz, Biezma Andres, Eickhoff Martin, Ezquirro Emilio, Fontela Pablo, Hennecke Klaus, Laing Doerte, Möllenhoff Marc, Nölke Marcus, Riffelmann Klaus-Jürgen, 2008. Direct steam generation in parabolic trough at 500 °C a German–Spanish project targeted on component and system design. In: 14th International Symposium on Concentrated Solar Power and Chemical Energy Technologies, SolarPACES.

ENEA. Website: Agenzia Nazionale per le Nuove Tecnologie, L'Energia e lo Sviluppo Economico Sostenibile (ENEA). ⟨http://www.enea.it⟩, Consulted in 2011.

Erdnic, O., Uzunoglu, M., 2012. Optimum design of hybrid renewable energy systems: overview of different approaches. Renewable and Sustainable Energy Reviews 16, 1412–1425.

Fernández-García, A., Zarza, E., Valenzuela, L., Pérez, M., 2010. Parabolic-trough solar collectors and their applications. Renewable and Sustainable Energy Reviews 14 (7), 1695–1721.

Grena, Roberto, Tarquini, Pietro, 2011. Solar linear fresnel collector using molten nitrates as heat transfer fluid. Energy 36 (2), 1048–1056.

Heller, Peter, Pfänder, Markus, Denk, Thorsten, Tellez, Felix, Valverde, Antonio, Fernandez, Jesús, Ring, Arik, 2006. Test and evaluation of a solar powered gas turbine system. Solar Energy 80 (10), 1225–1230.

Horn, Mechthild, Führing, Heiner, Rheinländer, Jürgen, 2004. Economic analysis of integrated solar combined cycle power plants: a sample case: The economic feasibility of an ISCCS power plant in Egypt. Energy 29 (5–6), 935–945.

Hosseini, R., Soltani, M., Valizadeh, G., 2005. Technical and economic assessment of the integrated solar combined cycle power plants in Iran. Renewable Energy 30 (10), 1541–1555.

Kaygusuz, Kamil, 2012. Energy for sustainable development: a case of developing countries. Renewable and Sustainable Energy Reviews 16, 1116–1126.

Klein, S.A., 2002. EES (Engineering Equation Solver) Manual. F-Chart Software.

Livshits, Maya, Kribus, Abraham, 2011. Solar hybrid steam injection gas turbine (stig) cycle. Solar Energy 86 (January (1)), 190–199.

Neij, L., 2008. Cost development of future technologies for power generation. A study based on experience curves and complementary bottom-up assessments. Energy Policy 36 (6), 2200–2211.

Novatec Solar, 2011. Novatec Solar Website. ⟨http://novatecsolar.com⟩.

Osuna, R., Fernández, V., Romero, S., 2004. PS10: A 11-MW solar tower power plant with saturated steam receiver. In: 12th SolarPACES International Symposium.

Papineau, M., 2006. An economic perspective on experience curves and dynamic economies in renewable energy technologies. Energy Policy 34 (4), 422–432.

Schwarzbözl, Peter, Buck, Reiner, Sugarmen, Chemi, Ring, Arik, Crespo, Ma Jesús Marcos, Altwegg, Peter, Enrile, Juan, 2006. Solar gas turbine systems: design, cost and perspectives. Solar Energy 80 (10), 1231–1240.

Solar Power and Chemical Energy Systems, SolarPACES, 2011. SolarPaces website: International Project Database. ⟨http://www.solarpaces.org/News/Projects/projects.htm⟩.

Suresh, M.V.J.J., Reddy, K.S., Kolar, Ajit Kumar, 2010. 4-e (energy, exergy, environment, and economic) analysis of solar thermal aided coal-fired power plants. Energy for Sustainable Development 14 (4), 267–279.

Williges, Keith, Lilliestam, Johan, Patt, Anthony, 2010. Making concentrated solar power competitive with coal: the costs of a European feed-in tariff. Energy Policy 38 (6), 3089–3097. (The Role of Trust in Managing Uncertainties in the Transition to a Sustainable Energy Economy, Special Section with Regular Papers).

Zarza Eduardo, 2003. Generación directa de vapor con colectores solares cilindro-parabólicos. Proyecto DIrect Solar Steam (DISS). Ph.D. Thesis, Escuela Superior de Ingenieros Industriales. Universidad de Sevilla, Julio.

Zarza, Eduardo, Rojas, Ma Esther, González, Lourdes, Caballero, José Ma, Rueda, Fernando, 2006. INDITEP: the first pre-commercial DSG solar power plant. Solar Energy 80 (10), 1270–1276.

Zhang, Yabei, Smith, Steven J., Kyle, G. Page, Stackhouse Jr., Paul W., 2010. Modeling the potential for thermal concentrating solar power technologies. Energy Policy 38 (12), 7884–7897. [Special Section: Carbon Reduction at Community Scale].